Numerical Solutions for the Lévêque Problem of Boundary Layer Mass or Heat Flux

Ekkehard Holzbecher

Weierstrass Institute for Applied Analysis and Stochastics (WIAS)
*Mohrenstr. 39, 10117 Berlin, GERMANY, holzbecher@wias-berlin.de

Abstract: The Lévêque problem is an idealized simple situation, concerning the influence of the boundary on the distribution of a heat or mass in Hagen-Poiseuille flow. The situation is relevant as an asymptotic case in several application fields, as heat transfer and chemical catalysis. Here the performance of numerical solutions is examined for a range of Péclet numbers, spanning 11 orders of magnitude. We examine the Sherwood, resp. Nusselt numbers and confirm the cubic square rule for high flow velocities. Moreover, we report on the effect of grid refinement and stabilization schemes.

Keywords: Heat and mass transport, Hagen Poiseuille flow, Lévêque solution, catalysis

1. Introduction

The problem, originally treated by Lévêque in 1928, describes an idealized situation, which appears in many application fields as a limiting case. It is worth to be examined, as it provides the possibility to relate measured results, numerical results and theoretical findings. It is especially the 1/3 power law (see below), which was stated by Lévêque (1928) that can be expected as an asymptotic for real world experiments - and also for numerical experiments.

The Lévêque problem is a flow and transport problem. There is laminar flow of a free fluid in the gap between two plates of constant spacing H. The problem can be reduced to 2D, with x-coordinate in flow direction, and y-direction perpendicular. A sketch of the set-up is given in Figure 1.

Concerning transport, one can either treat a thermal situation with heat transport (Ackerberg *et al*. 1978, Aydin & Avcia 2007), or a solute situation with mass transport (Phillips 1990). Lévêque (1928) was led to his research by the thermal situation. The inflowing fluid has a constant temperature in the thermal case or a constant concentration in the solute case. At one of the plates the fluid is cooled or heated to a temperature different from the inflow temperature.

In the solute case the analogous situation is given, when the solute reacts at the boundary to reach a constant concentration, different from inflow. Such a set-up is highly relevant in catalysis, when one of the walls is coated by a catalyst (Unwin & Compton 1989).

The simplifying assumption is made that the cooling or heating, or the reaction at the catalyst sites is infinitely fast, so that the wall temperature remains fixed. In the solute situation the solute is consumed completely, to reach a constant concentration of zero at the boundary. In the literature this is often referred to as *limit case*. For solute transport the limit case is given, if the reaction rate goes to infinity, i.e. if its characteristic time of the reaction exceeds the characteristic time scales of advection and diffusion.

The solution of Lévêque (1928) concerns the asymptotic regime for increasing velocities. The response of the system is the heat or mass transfer per unit width of the boundary. In dimensionless terms it is denoted by the Nusselt number Nu, for the thermal case, and the Sherwood number Sh, for the solute case. The classical result is denoted as

$$\mathrm{Sh} = 1.615 \left(\mathrm{Re} \cdot \mathrm{Pr}\, H / L \right)^{1/3} \qquad (1)$$

We can use this relationship in order to test numerical schemes. L denotes the length of the reaction zone (i.e. it's extension in flow direction), the Reynolds number $\mathrm{Re} = v_{max} H / \eta$ with maximum velocity v_{max} and fluid viscosity η and the Prandtl number $\mathrm{Pr} = \eta / D$ with diffusivity D. D denotes thermal diffusivity in the thermal case and solute (molecular) diffusivity in the solute case. The product of Reynolds- and Prandtl numbers is the Péclet number:

$$\mathrm{Pe} = \mathrm{Re} \cdot \mathrm{Pr} = \frac{v_{max} H}{D} \qquad (2)$$

2. Analytical Description

Using a Multiphysics Simulation Tool the flow and transport situation, described above, can be treated easily. For flow one can use the Navier-Stokes mode, as it is for example available in the base version of COMSOL. With a no-slip boundary condition at the walls, a prescribed velocity profile at the inlet and a zero pressure condition at the outlet, the flow field can be reproduced nicely, as long as the flow is laminar, i.e. the Reynolds number low enough.

However there is another alternative, which we prefer in this case. For the simple set-up in the Lévêque problem, there exists an analytical solution for the flow problem, which is the quadratic Hagen-Poisseuille profile. The profile is given by (see: Guyon *et al.* 1991)

$$v(y) = v_{max} \frac{4}{H} y \left(1 - \frac{y}{H} \right) \qquad (3)$$

with maximum velocity

$$v_{max} = -\frac{H^2}{8\eta} \frac{\partial p}{\partial x} \qquad (4)$$

Flow is in *x*-direction, along the boundaries, and *y* is directed perpendicular to the boundaries. *p* is the pressure variable, *H* denotes the height between the plates. The mean velocity is given by:

$$v_{mean} = \frac{2}{3} v_{max} = -\frac{H^2}{12\eta} \frac{\partial p}{\partial x} \qquad (5)$$

The flux per unit width is:

$$q = -\frac{H^3}{12\eta} \frac{\partial p}{\partial x} = H v_{mean} = \frac{2}{3} H v_{max} \qquad (6)$$

We use the analytical solution, in order to focus on the performance of the transport solver. Additional numerical errors due to the approximate solution of the flow problem are avoided in that way.

It was already stated that the problem can be conceived either as a solute or as a thermal problem. In the following we note the problem in terms of a solute concentration *c*, i.e. we describe the solute transport case. The differential equation for steady state transport is given by

$$\nabla D \nabla c = \mathbf{v} \nabla c \qquad (7)$$

with diffusivity *D* and velocity *v*. In the thermal case the thermal diffusivity needs to be considered in equation (7) instead of mass diffusivity. In dimensionless the transport equation takes the following form:

$$\nabla \nabla c = 4 y (1 - y) \mathrm{Pe} \nabla c \qquad (8)$$

At the electrode, located at one of the boundaries, we have the Neumann boundary condition:

$$D \frac{\partial c}{\partial n} = kc \qquad (9)$$

i.e. the diffusive flux is equal to the local reactive flux, described as product of reactive velocity *k* and concentration at the boundary. In dimensionless form equation (9) is written as:

$$\frac{\partial c}{\partial n} = \mathrm{Da} \cdot c \qquad (10)$$

with the dimensionless Damköhler number $\mathrm{Da} = k/D$. If the reaction is infinitely fast, we can assume that the concentration is reduced to 0 at the boundary, i.e. there is the Dirichlet boundary condition

$$c = 0 \qquad (11)$$

3. Model Set-up

We use COMSOL 'advection-diffusion' mode. A sketch of the model region is given in Figure 1. In the reference case the length of electrode boundary is 10 times larger than the channel height *H*. The length of undisturbed region at the inlet (black line at the bottom) is equal to the channel height. Thus the length of the catalyst layer in flow direction is *L*=9. For further scenarios, reported below, *L* is changed from the value of the reference case.
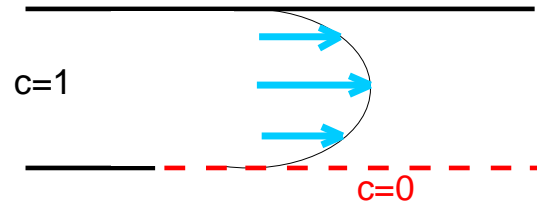

Figure 1. Sketch of the model set-up

Inflow concentration is *c*=1 (Dirichlet condition). There is another Dirichlet condition with *c*=0 at lower boundary for *x*>1. At all other closed boundaries the no flow condition is chosen. In COMSOL the outflow is characterised by the 'convective flux' condition, which is noted as:

$$\frac{\partial c}{\partial x} = 0 \qquad (12)$$

In the following we explore the effects of meshing. We use:

1. free triangular adaptive meshes, obtained by the default coarse grid with 2, 3 or 4 refinements
2. rectangular 'mapped meshes' (80 x 800 blocks; equidistant in *x*-direction, refined in *y*-direction; mesh growth factor 1.8.

Initial mesh (extra fine option) for the reference case has 3176 elements, corresponding to 14488 degrees of freedom (DOF).

We use default quadratic elements for all reported simulations. For all reference simulations we use the streamline diffusion stabilisation scheme with Petrov-Galerkin (compensated) and 0.25 as tuning parameter. Other stabilization methods, as they are implemented in COMSOL Multiphysics, as isotropic and anisotropic diffusion, or crosswind diffusion, did not perform as well as the chosen artificial diffusion method. For coarse meshes and high Péclet numbers the model did not converge without stabilisation. The effect of the stabilization, which for the Lévêque problem is also discussed by Naber and Koren (2007), is demonstrated below.

Calculations for the same model set-up, using a Finite Volume code, are published by Fuhrmann et al. (2008).

4. Results

The model was run for a set of Péclet numbers, stepping through 11 orders of magnitude, from a minimum of 0.001 to a maximum of 10^8.

Figure 2 shows the solutions for a selected set of Péclet numbers. For low Pe diffusion is dominant. The advective flux is not sufficient for a significant increase of the concentrations in the main part of the model region. Intermediate concentrations can mainly be recognized between the inlet and the border of the reactive boundary. Such behaviour is depicted in the uppermost sub-figure.

For high Pe advection is dominant and fluid with inflow concentration penetrates to the right. A boundary layer is established at the catalyst boundary, which becomes thinner with increasing Pe. In the lowermost sub-figure it is hardy recognizable.
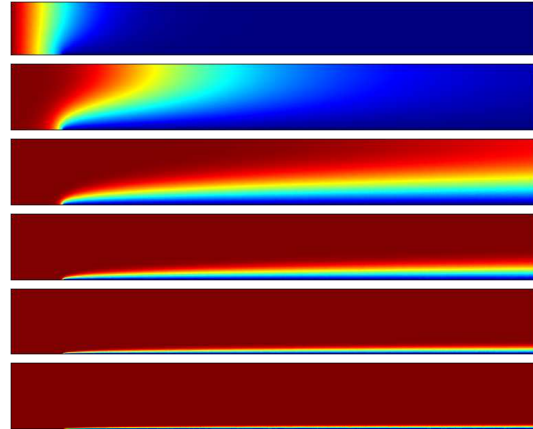

Figure 2. Concentration distributions for different Péclet-numbers; from top to bottom: Pe=0.1, 1, 10, 100, 1000, 10000; red represents inflow concentration (*c*=1), and blue the concentration at the catalyst boundary (*c*=0)

Between those two extremes, which we call low Pe and high Pe asymptotics in the sequel, a transition regime can be observed; best visualized in the second sub-figure of the shown sequence. This concentration distribution appears for Pe=1, where advective and diffusive fluxes are of equal importance.

The output characteristic of the system, which is of most interest, is the total mass transfer, i.e. the mass lost by the reaction at the boundary. Mass transfer per unit length is represented by the Sherwood number Sh, which is obtained by boundary integration along the electrode boundary. For the simulated set-up in the dimensionless formulation Sh is evaluated by:

$$\text{Sh} = \frac{1}{L}\int \frac{\partial c}{\partial y} dx \qquad (13)$$

The factor *D*, present in the general formulation, is neglected in formula (13). Note that for the thermal case the Nusselt number *Nu* takes the place of *Sh*.

In the following figures we provide Sherwood numbers in dependence of the Péclet numbers. Figure 3 shows the Pe-Sh diagram for the reference case. The two curves are obtained with different meshes. The free mesh provides inaccurate solutions for the two asymptotic states, while for the transition states the mass transfer is captured quite well by the coarse free mesh.
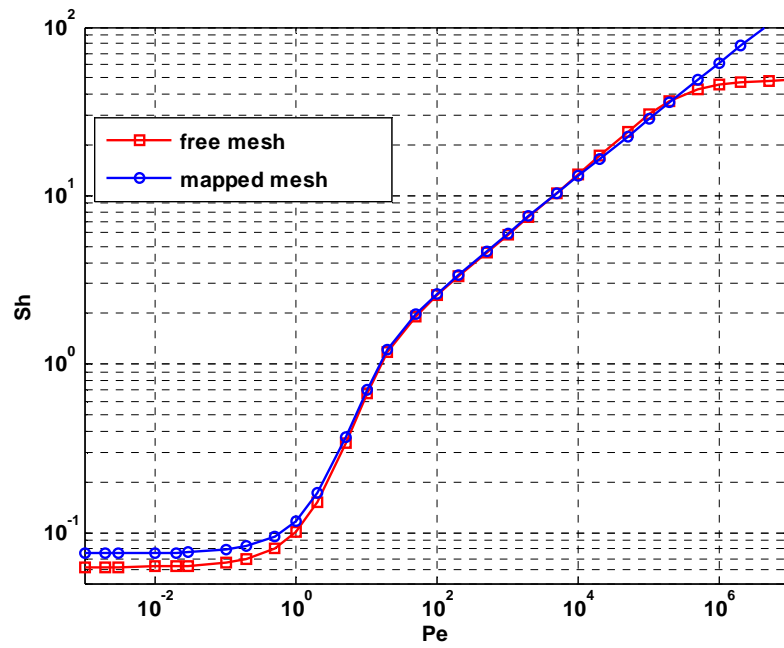
Figure 3. Péclet-Sherwood-number (*Pe-Sh*) diagram for length *L*=9, simulated using COMSOL, with coarse free mesh and mapped mesh
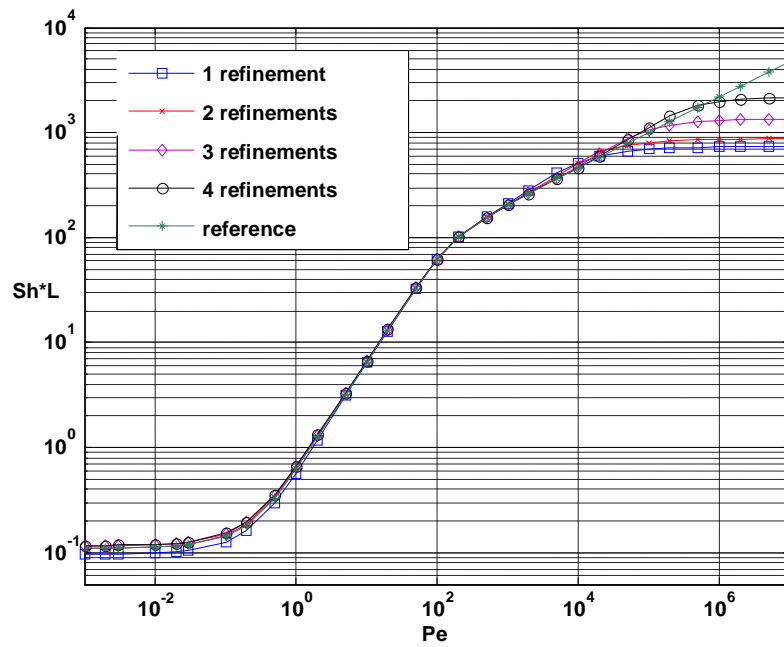

Figure 4. Péclet-Sherwood-number (*Pe-Sh*) diagram for length *L*=9, simulated using COMSOL; comparison of different free mesh refinements, reference is the mapped mesh solution with mesh

In Figure 4 we show the results of mesh refinement. Obviously the output of the mapped mesh run is approached by using refined free meshes. Degrees of freedom for the four refined meshes are: 57559, 229453, 916249, 3661873.

For the free mesh we also examined the performance of adaptive mesh refinement. Degrees of freedom in dependence of Péclet number for the reference situation are given in Table 1

Table 1: Degrees of freedom for default adaptive mesh refinement in dependence of the Péclet number, calculated with COMSOL 3.4

Pe	DOF after 1. refinement	DOF after 2. refinement
0.1	46720	125326
1	46693	122305
10	43837	114268
100	37924	99202
1000	36856	101974
10^4	40951	110032
10^5	43177	123433
10^6	43231	127339
10^7	42613	120868
10^8	42574	124858

We also examined the effect of the stabilisation. An impression is given in Figure 5, where the concentration profiles from four different runs (fine and coarse, with and without stabilisation) at the outlet are compared. For both meshes the use of the stabilisation leads to improved results, as the fluctuations are smaller and restricted to a smaller part of the profile. However for the coarser mesh still one over- and one under-shoot can be observed, even if stabilisation is applied. In the results for the fine grid these unphysical fluctuations have disappeared. Note that $Pe=10^6$ was the highest Péclet number, for which the model without stabilisation converged.

Also the influence of boundary length L on the Sherwood numbers was examined. Results for four different lengths and the varying Péclet number are given in the appendix. For low Pe the mass transfer per unit length, i.e. Sh, is approximately inverse proportional to L. This can be understood, because the major transfer occurs in the left part near the upstream margin of the reactive surface, while there is no transfer in the remaining part because of vanishing

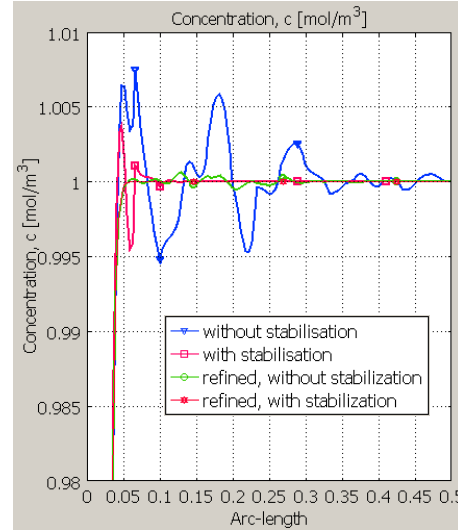concentration gradients. For high Pe the Sherwood number obeys the Lévêque 1/3 power law.

Figure 5. Effect of stabilization and refinement, demonstrated for $Pe=10^6$ and one or two refinements of the initial free mesh

Results for the kinetic reaction (see equation (10)), characterized by the Damköhler number Da in addition to Pe, are depicted in Figure 6. For low Da the non-dimensional mass transfer scales with the Damköhler number. For high Da, i.e. fast reactions, there is no influence, there is no influence of the mass transfer characteristic, as expected. The transition between these two asymptotic states occurs for $10^{-2}<Da<10^2$.
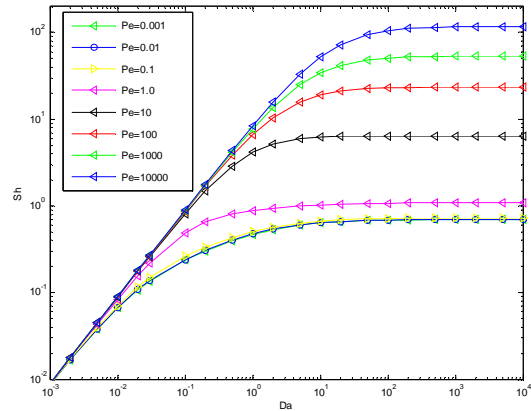

Figure 6. Mass transfer, characterised by the Sherwood number Sh, in dependence of Péclet number Pe and Damköhler number Da

5. Conclusions

For the Lévêque problem the comparison with the asymptotic solution enables a test of the numerical simulation.

Moreover the numerical model tells us more than theory: we can examine, which are the conditions to hold that the asymptotic is already valid.

- The Lévêque 1/3 power law is perfectly confirmed by the numerical results
- The transition between the two asymptotics appears for Péclet numbers between 0.3 and 30
- The mentioned transition regime is already captured accurately by coarse mesh simulations
- Mapped mesh simulations provide more accurate results than free mesh simulations
- For numerical methods it is a higher challenge to approximate the asymptotic situations than the transition regime

6. References

Ackerberg R.C., Patel R.D., Gupta S.K., The heat/mass transfer to a finite strip at small Péclet numbers, *J. Fluid Mech.* **86**(1), 49-65 (1978)

Aydin O., Avcia M., Analysis of laminar heat transfer in micro-Poiseuille flow, *International Journal of Thermal Sciences* **46**(1), 30-37 (2007)

Fuhrmann J., Zhao H., Holzbecher E., Langmach H., Chojak M., Halseid R., Jusys Z., Behm R.J., Numerical calculation of the limiting current in a channel flow cell with a circular electrode, *Phys.Chem. & Chem. Phys.*, to appear (2008)

Guyon E., Hulin J-P., Petit L., Hydrodynamique Physique, Ed. du CNRS (1991)

Lévêque A., Les lois de la transmission de chaleur par convection, *Ann. des Mines* **13**, 201-299, 305-362, 381-415 (1928)

Naber J., Koren B., Towards an h-adaptive immersed boundary method for unsteady incompressible Navier-Stokes equations, Report MAS-E0705, Centrum for Wiskunde en Informatica, 21p (2007)

Phillips C.G., Heat and mass transfer from a film into steady shear flow, *Quat. Journal Mech. Appl. Math.* **43**(1), 135-159 (1990)

Unwin P.R., Compton R.G., The determination of heterogeneous kinetics using the channel electrode, *J. Electroanal. Chem.* **274**, 249-256, 1989

7. Acknowledgements

8. Appendix

Table 2: Sherwood numbers Sh, calculated for different Péclet numbers Pe and lengths L

Pe	L=9	L=18	L=36	L=72
0	0.67536			
0.001	0.67569	0.39444	0.2134	0.10978
0.002	0.67601	0.39477	0.21372	0.11009
0.005	0.67634	0.39509	0.21404	0.1104
0.01	0.67864	0.39736	0.21628	0.1126
0.02	0.68194	0.40062	0.2195	0.11578
0.05	0.68524	0.4039	0.22275	0.11902
0.1	0.7087	0.42737	0.24643	0.14335
0.2	0.74319	0.46243	0.28293	0.1829
0.5	0.8534	0.57829	0.41045	0.32993
1	1.059	0.80459	0.67177	0.62648
2	1.5428	1.3526	1.2866	1.262
5	3.326	3.2776	3.2519	3.2178
10	6.3683	6.5832	6.5639	6.5207
20	10.943	12.784	13.19	13.156
50	17.8	25.195	31.007	32.947
100	23.449	35.581	50.415	62.066
200	30.257	46.867	71.163	100.87
500	41.914	65.547	101.88	156.21
1000	53.376	83.815	131.11	203.8
2000	67.793	106.75	167.65	262.25
5000	92.731	146.38	230.68	362.63
10^4	117.35	185.49	292.81	461.41
$2 \cdot 10^4$	148.36	234.73	371.02	585.66
$5 \cdot 10^4$	202.04	319.96	506.35	800.58
10^5	255.05	404.12	639.95	1012.7
$2 \cdot 10^5$	321.84	510.14	808.26	1279.9
$5 \cdot 10^5$	437.47	693.7	1099.7	1742.5
10^6	551.67	874.97	1387.4	2199.3
$2 \cdot 10^6$	695.56	1103.4	1750	2774.8
$5 \cdot 10^6$	944.74	1498.9	2377.7	3771.3
10^7	1190.9	1889.5	2997.7	4755.5
10^8	2476.6			